This is a repository copy of *An In Silico Study on the Isomers of Pentacene: the Case for Air-Stable and Alternative C22H14 Acenes for Organic Electronics*.

White Rose Research Online URL for this paper:
http://eprints.whiterose.ac.uk/114179/

Version: Accepted Version

1
2
3
4
5
6
7
8
9
10
11
12
13
14
15
16
17
18
19
20
21
22
23
24
25
26
27
28
29
30
31
32
33
34
35
36
37
38
39
40
41
42
43
44
45
46
47
48
49
50
51
52
53
54
55
56
57
58
59
60

An *In Silico* Study on the Isomers of Pentacene: the Case for Air-Stable and Alternative $C_{22}H_{14}$ Acenes for Organic Electronics

Leighton Jones and Long Lin*

Centre for Industrial Collaboration, School of Chemistry, University of Leeds, Woodhouse Lane, Leeds, West Yorkshire, UK, LS2 9JT

Abstract: Pentacene is one of the most investigated candidates for organic thin film transistor (OTFT) applications over the last few decades even though it unstable in air (E_g = 1.80 eV), owing in part to its planar nature and high charge-transfer mobilities as both a single crystal (35 cm^2 V^{-1} s^{-1}) and as a thin-film (3.0 cm^2 V^{-1} s^{-1}). Until now, picene is the only isomer of pentacene to be investigated for organic electronic applications, due to its greater stability (E_g = 4.21 eV) and high-charge transfer mobility (3.0 cm^2 V^{-1} s^{-1}); even benefitting from oxygen doping. In the present study, a total of twelve fused-ring isomers (including pentacene, picene and ten other structures) of the formula $C_{22}H_{14}$ were analyzed and investigated for their electronic and optical properties for worth in OTFT applications. We screened several pure and hybrid DFT functionals against the experimental frontier molecular orbitals (FMOs) of pentacene, then deployed Marcus Theory, Koopmans' Theorem and Green's function with the P3 electron propagator variant, for the internal hole reorganization energy, the hole transfer integral (*via* the 'splitting-in-dimer method' at *d*=3.0, 3.5 and 4.0 Å),

1

the charge transfer rate constant and vertical ionization energies. Using these as a basis, we studied pentacene's isomers and found that the four non-planar structures, namely benzo[g]chrysene (**3**), naphtho[c]phenanthrene (**7**), benzo[c]chrysene (**11**) and dibenzo[c,c']phenthrene (**12**), are (I) more stable than pentacene, by up to 2 eV, and (II) have relatively similar ionization energies (7.5-7.6 eV) to those of picene's experimental value (7.51 eV). The largest charge transfer rates at 3.5 Å dimer separations were given by the isomers benzo[b]chrysene **4**, naphtha[c]phenanthrene **7**, dibenzo[a,c]anthracene **8** and benzo[a]tetracene **10** and found to be 2.92, 1.72, 1.30 and 3.09×10^{14} s^{-1} respectively. In comparison to that of pentacene ($K_{CT} = 3.97 \times 10^{14}$ s^{-1}), these unusual isomers are thus promising air-stable and alternative candidates for organic electronic applications.

I. INTRODUCTION

There has been great progress in the fields of materials chemistry and engineering in the last few decades for high-performing small-molecule charge-transfer materials[1-4], as the active component in opto-electronic devices which include light emitting diodes, photovoltaics and flexible display screens[5-9]. Charge-transfer materials need to overcome a number of diverse issues and further satisfy the increasing demand of greater performance, driven both by commercial growth and scientific inquest. Such macroscopic issues include industrial-scale device fabrication, the ease of processing each individual component layer, and overall device performance. While these are highly important, there are a number of microscopic issues at the molecular level which have yet to be addressed, and include air stability for ambient condition processing and efficient charge transfer across the active layer. Thus, suitable molecular structures are needed to bring together all the above concepts and provide the next generation of candidates for high-performing properties and device outputs.

2

Polycyclic aromatic hydrocarbons (PAHs) have been extensively investigated as organic semiconductors (OSCs) for the active layer in organic electronic devices. These are found to satisfy a large number of the above issues, yet there are few which have both air-stability and high charge-transfer properties. One line of inquiry is the investigation of the charge transfer mechanisms[11-12] for the improvement of organic-based devices. These investigations tend to focus on single-crystal OSC devices, where charge transfer mobility can reach as high as 35 cm^2 V^{-1} s^{-1} with a PAH molecule called pentacene[13-17]. Pentacene (**1**, Figure 1) is comprised of five fused benzene rings in a linear array of only carbon and hydrogen atoms.

1   **2**
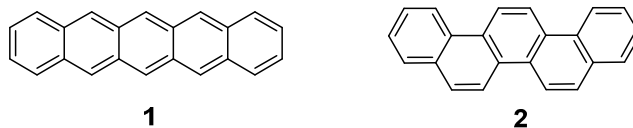
Figure 1. Structures of pentacene (**1**) and picene (**2**).

Single crystals of OSCs are commonly used because of their close-packing continuum of the organic molecules in the solid phase. On the other hand, the OSCs applied to organic electronics are in a thin-film state and do not necessarily obey the same charge transport conduction mechanisms[18], even though they can still reach high transport mobilities, such as 3.0 cm^2 V^{-1} s^{-1} with a thin-film transistor of pentacene[15,19]. For this reason, more fundamental investigations, based solely on their molecular structures and not on the device architecture, are needed.

It was found that pentacene gave different values for the same charge-transfer and optoelectronic properties, depending on the applied experimental conditions. It was soon evident that pentacene is unstable in air[4] due to its small HOMO-LUMO gap ($E_g = 1.8$ eV), so is easily oxidised and difficult to operate under ambient conditions. Picene, an isomer of

3

pentacene (**2**, Figure 1), is surprising in the sense that its charge transport benefits from oxygen doping[20-22], which is a well-known p-type doping phenomenon[23-25] with other OSCs. This suggests that picene with E_g = 4.21 eV has a superior stability over pentacene, imparted only from its molecular structure. Although this was further explored through both experimental observations and theoretical calculations[22,26], the studies, however, focused on the charge-transfer properties of just these two isomers alone. There are twelve known isomers of (and including) pentacene[27-29], which have the formula $C_{22}H_{14}$. It is thus reasonable to continue this long line of investigation and probe the properties of the other isomers.

So far, their structures have only been explored with regards to their size[27] and aromatic nature[28,29]. To date, there are no known studies on the fundamental electronic and optical properties of the isomers of pentacene, even though there are reports of some being successfully synthesized, but not subjected to charge-transfer investigations[30,31]. The identification and characterization of these isomeric structures is paramount to develop this set of $C_{22}H_{14}$ PAHs and more importantly, determine which isomers are best suited for acene-based small-molecule technology.

This can be investigated with computational chemistry, where electronic and optical properties can be adequately modelled using a combination of molecular and quantum mechanics. Generally, a range of theories are tested and compared with experimental observations where possible or other theoretical calculations in the literature, then one is selected and applied to a wider range of structures. This approach has huge merit for materials chemistry and particularly small-molecule organic electronic devices, as large numbers of structures can be effectively screened for the active layer prior to any synthetic work undertaken and subsequently minimizes both the resources and the time used in

4

synthetic endeavors, as structures predicted to have high-performing properties can be specifically targeted out of a pool of potential candidates.

Herein, this present work deploys different theories which include density functional theory (DFT), Koopman's Theorem and Green's Function to calculate the physical properties of these isomers and identify suitable isomers as alternative candidates for the improvement of (1) their stability relative to pentacene, and (2) high charge-transfer properties for organic electronics. We start by investigating their stability by predicting the HOMO-LUMO gaps and ionization energies of the twelve isomers and then probe their charge-transfer properties through the Marcus Theory, which involves the calculation of their internal reorganization energies and using the 'splitting-in-dimer' method to calculate the transfer integrals across three intermolecular separations (d = 3.0, 3.5 and 4.0 Å); these parameters enable the rates of charge transfer to be determined and thus a deep understanding of the suitability of the isomers for organic electronic applications in comparison to pentacene. This study presents evidence that suggests the theoretical assessment of a leading target's isomers is a worthy pursuit prior to synthetic investigations to uncover new candidates for high-performing structures and highlight those which may have improved properties.

5

II. THEORETICAL AND COMPUTATIONAL METHODS

All structures were drawn and visualized in Avogadro (version 1.1.1)[32]. The ground-states of the molecular structures were first optimized in Avogadro with the molecular mechanics universal force field (UFF), then optimized with quantum mechanics at the given theoretical level using density functional theory (DFT), or time-dependent density functional theory (TD-DFT) for the excited-state calculations, in Gaussian 09 (version D.01)[33]; all subsequent single-point DFT calculations for the charge transfer properties were performed in Gaussian 09 starting with the optimized structure at the same level of theory.

For the benchmarking section, a molecule of pentacene was individually optimized with each functional, and found to be a minimum with frequency calculations, *i.e.* no imaginary frequencies were observed – see ESI† for the infrared spectra calculated with each functional, and the spectra for all isomers investigated later in this study; the vibrational frequencies of pentacene correlate well with the literature[34,35].

Several DFT functionals were screened against the experimental values of pentacene and probed some charge-transfer interactions, as shown in Tables 1 and 2; these functionals include pure (BLYP, PBE) and hybrid (B3LYP, wB97XD, PBE0, B3P86, BHandH, BHandHLYP) with long-range corrections (LC and CAM) and Grimme's dispersion (D3). The properties include the HOMO, LUMO, E_g, first vertical ionization energy (IE_V), reorganization energy, transfer integral and rate of charge transfer. Both pure and hybrid functionals were included, along with long-range correction (LC/CAM) and Grimme's third order dispersion (D3) factor. The ionization energy was probed with Koopmans' Theorem[50-52] (KT), outer valence Green's function[53-55] (OVGF), and a variant, the third-order electron propagator[56-59] (P3).

6

Although the 6-31G(d) and 6-31+G(d) basis sets have been found to give satisfactory values to experimental observations[36-39], more-complete basis sets such as of 6-311G to 6-311++G(d,p) are also prevalent throughout the literature[40-43] for higher accuracy where needed. We also deploy the 6-311++G(d,p) basis set, owing to the unknown structures and charge transfer properties of the isomers of pentacene, particularly with regards to the dimer separations of the non-planar isomers, which do not have experimental observations for comparison with this work.

Marcus Theory[44] (Equation 1), was used to describe the charge transfer, which is as a self-exchange between a neutral and a charged molecule. Two key parameters, the internal hole reorganization energy (λ_h)[45], which is intrinsic only to the extent of relaxation between the neutral and cationic surfaces and upon which, the electron delocalization of a molecular geometry plays a key part, and the hole transfer integral (t_h), which is the electronic coupling between the molecules in relation to the intermolecular separations between them. K_B is Boltzmann's constant, T is temperature (298.15 K used here) and $\hbar$ is the reduced Planck's constant. Ideally, internal reorganization energies should be very small[46], $ca.$ 0.1 eV.

$$k_{ct} = \left(\frac{t^2}{\hbar}\right)\left(\frac{\pi}{\lambda_{\pm} k_B T}\right)^{1/2} e^{\frac{\lambda_{\pm}}{4 k_B T}} \quad (1)$$

A vertically ionized or reduced state is the immediate nature of a molecule which has gained or lost an electron and an adiabatic state is where the vertical state has subsequently relaxed to a minima on its potential energy surface. The energy processes of electron-exchange, excitation and relaxation are illustrated in Figure 2.

7
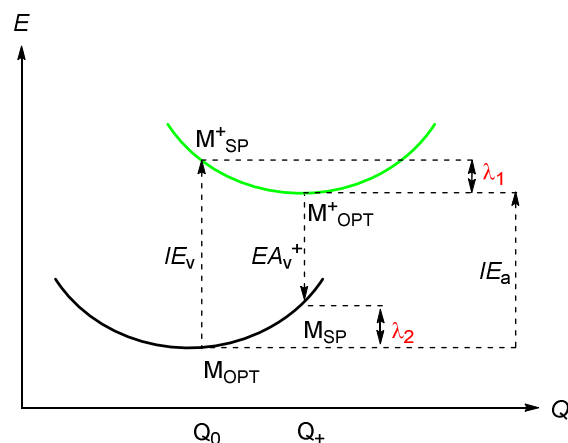
Figure 2. The ionization energy (*IE*) and electron affinity (*EA*) pathways between the neutral (black) and cation (green) potential energy surfaces for the calculation of the hole reorganization energy λ_h.

The internal hole reorganization energy (λ_h) is comprised of two relaxation terms, the energy of the cationic (λ_1) and neutral (λ_2) surfaces, as defined in Equation 2.

$$\lambda_h = \lambda_1 + \lambda_2 \qquad (2)$$

The cationic reorganization energy λ_1 is determined from the difference between the vertical and adiabatic ionization energies calculated *via* the vertical, single-point geometry of the cation (M^+_{SP}) and the optimized cation structure (M^+_{OPT}), (Equation 3).

$$\lambda_1 = E(M^+_{SP}) - E\left(M^+_{opt}\right) \qquad (3)$$

Addition of an electron to the minimized cationic structure returns the molecule back to its neutral potential energy surface and is performed with a vertical electron affinity of the cation, EA_v^+; the difference between this state and the minimum of the neutral molecule is λ_2 (Equation 4).

$$\lambda_2 = E(M_{SP}) - E(M_{OPT}) \qquad (4)$$

The hole transfer integral t_h is an important component in Marcus Theory and can be estimated from the 'splitting-in-dimer' method[36,42,47,48] (Equation 5), comprising of two cofacial molecules separated by a distance d (Å) and determined from calculating half the

8

energy difference between the HOMO and HOMO-1 levels of the dimer. The transfer integral decreases with increasing d, so a range of separations are appropriate to determine the extent of the electronic coupling interaction. Although a separation between d=3.3-3.8 Å was found to be suitable for OSCs such as pentacene[48], circum(oligo)acenes[36], and substituted acenes[43], it is reasonable to assume that not all of the other isomers in this study, some being non-planar, will have an identical packing arrangement, and thus three integrals were calculated at 3.0, 3.5 and 4.0 Å.

$$t_h = \frac{1}{2}(\Phi_H - \Phi_{H-1}) \qquad (5)$$

Substituting values for λ_h and t_h into Equation 1, enables K_{CT} to be determined at any given separation d.

II.I FUNCTIONAL SELECTION

Different DFT functionals were screened against pentacene's FMO experimental properties, with other theories such as KT, OVGF and P3 deployed for comparison of the vertical ionization energy. The charge-transfer properties, such as the internal reorganization energy, transfer integral and rate of charge transfer, were then calculated and compared to experimental and theoretical literature values. Table 1 shows the hybrid functionals B3LYP and PBE0, which gave the closest HOMO, LUMO and E_g energies in comparison to the experimental energies[60,61] of -5.00 eV, -3.20 eV and 1.80 eV respectively, although the B3P86, BHandH and BHandHLYP functionals were off by more than 0.5 eV. While the pure functionals BLYP and PBEPBE proved exceptionally poor, the worst performing functionals were those of the long-range corrected or range-separated hybrids, namely LC-BLYP, LC-ωPBE, CAM-B3LYP and ωB97XD, with differences to experiment between 1-2 eV.

In stark contrast, the long-range corrected functionals gave some of the closest values to the experimental first vertical ionization energy[62] of 6.59 eV, with LC-BLYP and LC-ωPBE

9

proving the most accurate, except for CAM-B3LYP which has a difference of 0.76 eV. Interestingly, the ωB97XD gave a close under estimation of 6.42 eV, while the hybrid B3P86 over estimates at 6.84 eV. The widely-used Koopmans' Theorem underperformed by 0.53 eV, similar to the BLYP functional. The outer valence Green's function gave relatively similar values to the hybrid functionals B3LYP and PBE0, while the third order electron propagator, P3, was the most accurate, slightly beating LC-BLYP, at 6.51 eV.

Table 2 shows the calculated internal hole reorganization energies (λ_h), hole transfer integral (t_h) and the rate of charge transfer (K_{CT}) for each functional; Grimme's third-order dispersion (D3) term were added for comparison of the intermolecular interactions. The lowest reorganization energy were found with BLYP and PBEPBE (61 meV), followed closely by B3P86 (94 meV) and B3LYP (97 meV), which correlate well with both the experimental value[62] of 59 meV and theoretical calculations[39,48,63]. PBE0 gave a similar energy, 106 meV, while other hybrid functionals such as ωB97XD, BHandH and BHandHLYP are relatively higher at 171, 159 and 176 meV respectively. The largest reorganization energies for pentacene were obtained with the long-range corrected functionals, including LC-BLYP (291 meV), CAM-B3LYP (189 meV) and LC-ωPBE (265 meV).

The spacing of d = 3.3-3.8 Å are reported in the literature[36,48,64] to be suitable for the transfer integrals of OSCs such as pentacene, although here we calculate d for 3.0, 3.5 and 4.0 Å to determine how the functionals affect the electronic coupling over a range of intermolecular separations. The first trend is the depreciation of both the transfer integral and the rate constant with increasing dimer spacings, across the range of functionals used, in agreement with the literature[48]. This is natural, as the intermolecular distances increase, *i.e.* the molecules in the dimer become further separated, their electronic coupling decreases and

10

thus charge transfer would diminish. With each 0.5 Å increment, the hole transfer integrals

decrease exponentially[48]

Table 1. HOMO, LUMO, E_g and Vertical Ionization Potential IE_v of Pentacene, in Electron Volts (eV) with Various Functionals[a]

Functional	HOMO	LUMO	E_g	IE_v
BLYP	-4.26	-3.12	1.15	5.99
LC-BLYP	-7.16	-0.75	6.41	6.65
B3LYP	-4.94	-2.75	2.19	6.23
CAM-B3LYP	-6.04	-1.70	4.33	5.83
LC-ωPBE	-7.12	-0.89	6.23	6.65
PBEPBE	-4.45	-3.31	1.15	6.18
PBE0	-5.09	-2.64	2.45	6.27
ωB97XD	-6.57	-1.14	5.43	6.42
B3P86	-5.55	-3.36	2.19	6.84
BHandH	-5.57	-1.77	3.80	6.17
BHandHLYP	-5.59	-1.75	3.84	6.16
KT				6.06
OVGF				6.25
P3				6.51
Experimental	-5.00	-3.20	1.80	6.59

[a]Basis set 6-311++G(d,p)

for the BLYP functionals, from 416 meV at 3.0 Å through 315 meV at 3.5 Å to 144 meV at

4.0 Å. Interestingly, there is little interaction of the Grimme's third-order dispersion across

the dimer separations $d = 3.0$-4.0. The wB97XD, B3P86, BHandH and BHandHLYP

11

functionals have exceedingly high hole transfer integrals for $d = 3.0$ Å at 804, 633, 764 and 745 meV respectively, similar to the long-range functionals such as LC-BLYP (826 meV), CAM-B3LYP (790 meV) and LC-ωPBE (806 meV). The majority of the hybrid functionals give relatively lower hole transfer integrals around 345-350 Å. Moreover, the integrals at 4.0 Å range between 140 and 190 meV for the uncorrected pure and hybrid functionals; interestingly that of B3LYP has excellent correlation with thin-film studies[65].

The charge-transfer rate constants are of the order 0.014-1.963×10^{15} s^{-1} for the dimer distances $d = 3.0$-4.0 Å and functionals investigated in agreement with the literature[36,48]. The rates calculated at the 3.0 Å spacing were found to be relatively lower with long-range corrected functionals such as LC-BLYP ($K_{CT} = 0.199 \times 10^{15}$ s^{-1}) and CAM-B3LYP ($K_{CT} = 0.610 \times 10^{15}$ s^{-1}) than uncorrected pure BLYP ($K_{CT} = 1.04 \times 10^{15}$ s^{-1}) and hybrid B3LYP ($K_{CT} = 1.30 \times 10^{15}$ s^{-1}) respectively; this trend is reproducible with increasing d. The transfer integrals for long-range functionals approximately halve with each 0.5 Å angstrom increment, inferring a linear dependency, but the uncorrected pure and hybrid functionals show exponential decreases in accordance with the literature[48]. Having screened pentacene's properties with various functionals, it is apparent that neither dispersion nor long-range functionals are appropriate for further investigations but rather the best performing one was B3LYP in correlation with the literature[36,48,64] and therefore selected for the calculation of the electronic and optical properties of the remaining isomers.

12

Table 2. Internal Hole Reorganization Energy (λ_h / meV), Hole Transfer Integral (t_h / meV) and the Rate of Charge Transfer ($K_{CT} \times 10^{15}$ / s^{-1}) for Each Functional at d=3.0, 3.5 and 4.0 Å Dimer Spacings for Pentacene

Functional	λ_h	d=3.0 Å		d=3.5 Å		d=4.0 Å	
		t_h	K_{CT}	t_h	K_{CT}	t_h	K_{CT}
BLYP	61	416	1.04	315	0.595	144	0.124
BLYP-D3	61	418	1.04	315	0.594	144	0.124
LC-BLYP	291	826	0.199	419	0.051	200	0.012
B3LYP	97	624	1.30	345	0.397	159	0.084
B3LYP-D3	97	625	1.30	345	0.397	159	0.084
CAM-B3LYP	189	790	0.610	381	0.142	180	0.032
CAM-B3LYP-D3	169	791	0.786	381	0.183	180	0.041
LC-ωPBE	265	806	0.256	399	0.063	185	0.014
LC-ωPBE-D3	265	806	0.256	399	0.063	185	0.014
PBEPBE	61	413	1.02	315	0.592	142	0.120
PBEPBE-D3	61	414	1.03	315	0.592	141	0.120
PBE0	106	654	1.25	351	0.362	160	0.075
PBE0-D3	106	655	1.25	351	0.362	160	0.075
ωB97XD	171	804	0.791	383	0.179	181	0.040
B3P86	94	633	1.40	345	0.416	156	0.085
BHandH	159	764	0.832	404	0.233	190	0.051
BHandHLYP	176	745	0.638	176	0.176	183	0.039

13

III. RESULTS AND DISCUSSION

The twelve known isomers of pentacene are illustrated in Figure 3, with selected bond lengths and angles. Their shapes vary from linear (pentacene, isomer **1**) to phenacene-like (picene, isomer **2**). Isomers benzo[*g*]chrysene **3** and dibenzo[*a,c*]anthracene **8** have a phenacene-like backbone with a phenyl ring appended in a *sec* and *tert* arrangement, respectively. The remaining isomers **4**-**7** and **9**-**12** have an end-on-end linear-array of phenyl rings, which includes the nonplanar structures benzo[*c*]chrysene **11** and dibenzo[*c,c'*]phenanthrene **12**. Isomer **12** is unusual, as it is a primitive or a 'half' helicene, making it a distinctive non-planar structure; there are four nonplanar structures in total, namely isomers **3**, **7**, **11** and **12**, as illustrated in Figure 4. **3** has a saddle-horse type structure, **7** and **11** have out-of-plane phenyl rings and **12** is half helical.

It is important to note the arrangements of the phenyl rings and the separation between the adjacent C-H units[49]. For example, pentacene has a zig-zag motif imparted by a 1,3 C-H arrangement, whereas picene has a chair motif from a 1,4 C-H arrangement. Structures which have 1,5 (**3**, **11**) or 1,6 (**12**) arrangements are found, as expected, to be non-planar, due to steric hindrance.

14

Pentacene

1

Picene

2

Benzo[*g*]chrysene

3

Benzo[*b*]chrysene

4

Dibenzo[*a,h*]anthracene

5

Dibenzo[*d,d'*]phenanthrene

6

Naphtho[*c*]phenanthrene

7

Dibenzo[*a,c*]anthracene

8

Dibenzo[*a,f*]anthracene

9

Benzo[*a*]tetracene

10

Benzo[*c*]chrysene

11

Dibenzo[*c,c'*]phenanthrene

12
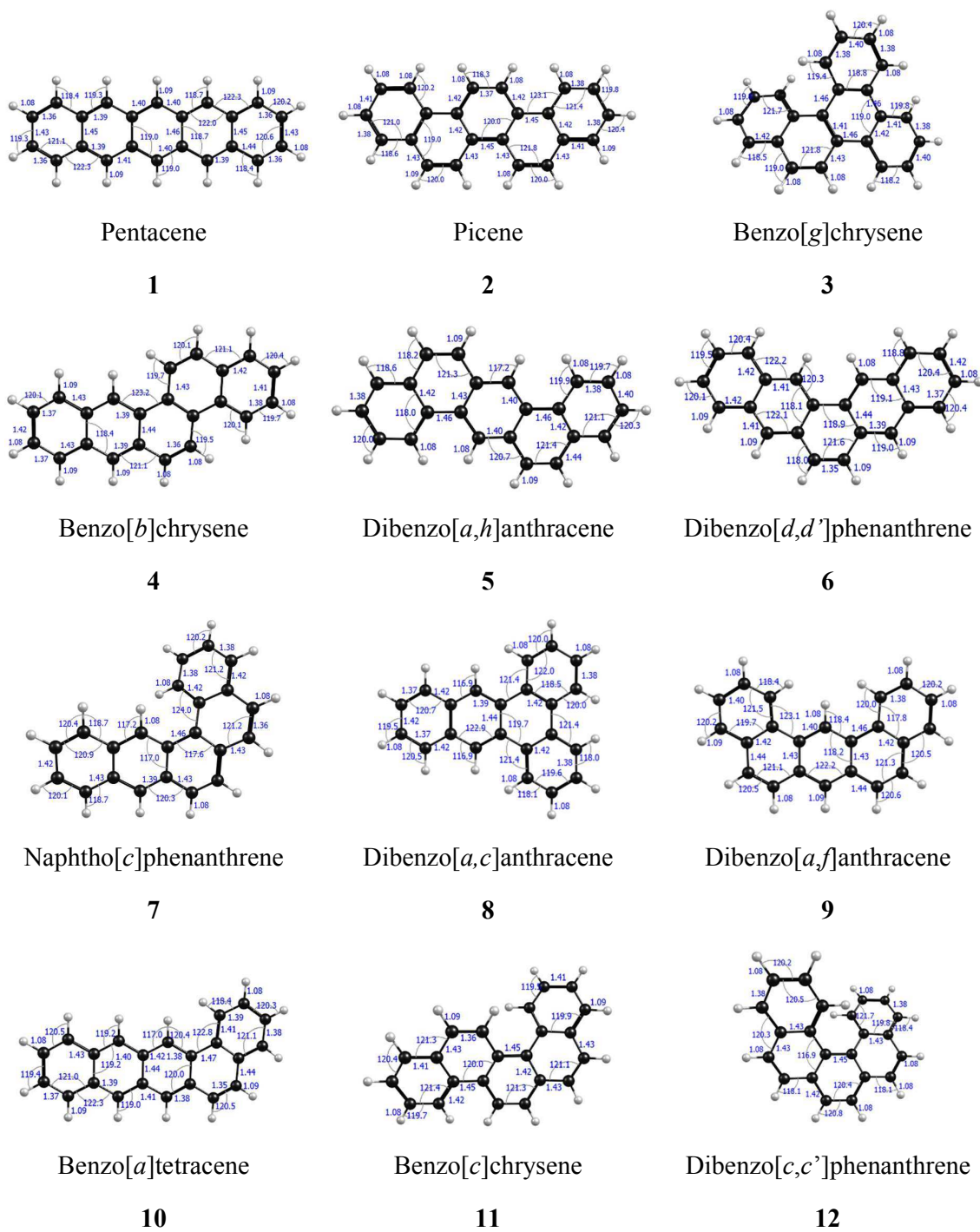
Figure 3. Structures of the 12 isomers investigated in this work with selected angles (°) and bond lengths (Å).

15

Benzo[g]chrysene

3

Naphtho[c]phenanthrene

7

Benzo[c]chrysene

11

Dibenzo[c,c']phenanthrene

12
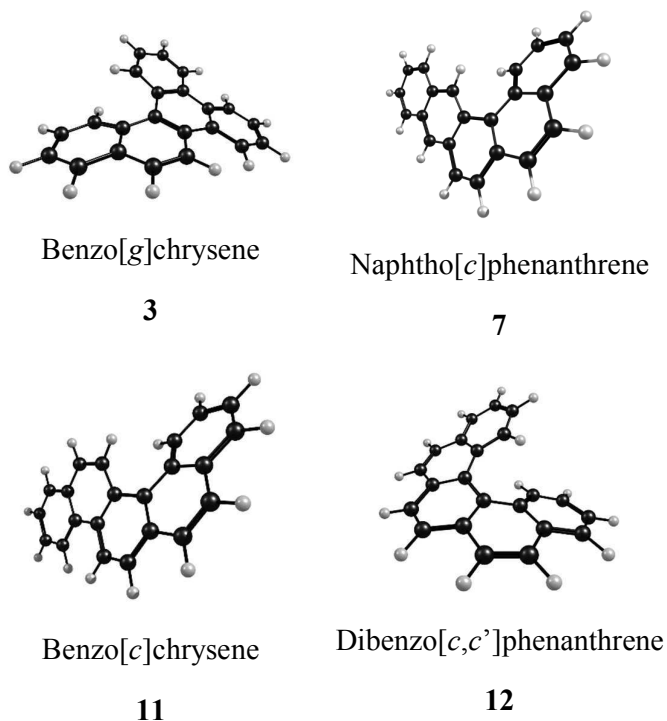
Figure 4. Structures of the four non-planar isomers.

The HOMO energy of pentacene (-4.94 eV) is the highest out of all the isomers studied (Table 3); the relatively high HOMO energy is a known issue, which is considered to contribute to its instability[22,26]. By rearranging just one of the terminal rings, isomer **10** shows a relatively similar HOMO energy at -5.29 eV but significant improvement in stability, as evidenced by an increase in both the E_g and the optical gap energies, by more than 0.6 and 0.69 eV respectively; however **10** is the second least stable after pentacene out of all the isomers.

Other than picene, the remaining planar isomers **4-6** and **8** and **9** also have significantly improved stability and deeper HOMO levels than pentacene. Isomer **9** is one of the most stable planar structures (E_g = 3.89 eV) excluding picene; followed closely by isomers **5** and **8**, which have the same gap (E_g = 3.85 eV).

16

The FMO energies of the non-planar **3**, **11** and **12** isomers are relatively similar to those of

picene (**2**), with their deep HOMO levels centered at -5.85 eV, the LUMO at 1.70 eV and the

Table 3. HOMO, LUMO, E_g, Optical Gap (S_0-S_1) with the Oscillator Strength in Parenthesis of the Optimized Isomers at the B3LYP/6-311++G(d,p) level, in electron volts eV

Isomer	H-1	H	L	L+1	E_g	S_0-S_1
1	-6.22	-4.94	-2.75	-1.33	2.19	1.90 (0.04)
2	-6.12	-5.85	-1.64	-1.59	4.21	3.55 (0.006)
3	-6.21	-5.80	-1.75	-1.38	4.05	3.60 (0.02)
4	-6.32	-5.55	-2.07	-1.32	3.48	3.10 (0.07)
5	-6.12	-5.72	-1.87	-1.56	3.85	3.36 (0.02)
6	-5.82	-5.66	-1.92	-1.90	3.75	3.11 (0.002)
7	-6.17	-5.52	-2.10	-1.36	3.42	3.02 (0.04)
8	-6.25	-5.76	-1.91	-1.32	3.85	3.43 (0.02)
9	-6.04	-5.76	-1.87	-1.56	3.89	3.38 (0.0004)
10	-6.28	-5.29	-2.37	-1.32	2.92	2.59 (0.04)
11	-5.95	-5.88	-1.67	-1.67	4.21	3.43 (0.002)
12	-5.97	-5.84	-1.72	-1.69	4.12	3.35 (0.001)

E_g at 4.2 eV; **7** is the exception with values -5.52, -2.10 and 3.42 eV respectively, but not

far from ideal. The HOMO-1 states for isomers **1** to **5** and **7** to **10** are relatively similar,

focusing around -6.20 eV, suggesting this is a common and stable lower FMO energy;

although no distinct trend is observed with the LUMO+1 states. The FMO levels are

illustrated in Figure 5 and clearly shows the trends in stability between the planar and non-

planar isomers. The molecular orbital plots are presented in Table S78 in the ESI† showing

the differences between the pentacene and phenacene-like structures, which correlate well

with the literature[66-69].

These trends are reflected in the optical gap (S_0-S_1 / eV), determined from TD-DFT calculations. The excitation wavelengths of **5**, **8**, **11** and **12** are nearly doubled in comparison to pentacene (3.35-3.43 eV). **4** and **6** have moderate stability (3.10-3.11 eV), while the lowest is with isomer **10** at 2.59 eV. Interestingly, the non-planar isomer **3** is the most stable, more than picene by 0.05 eV.
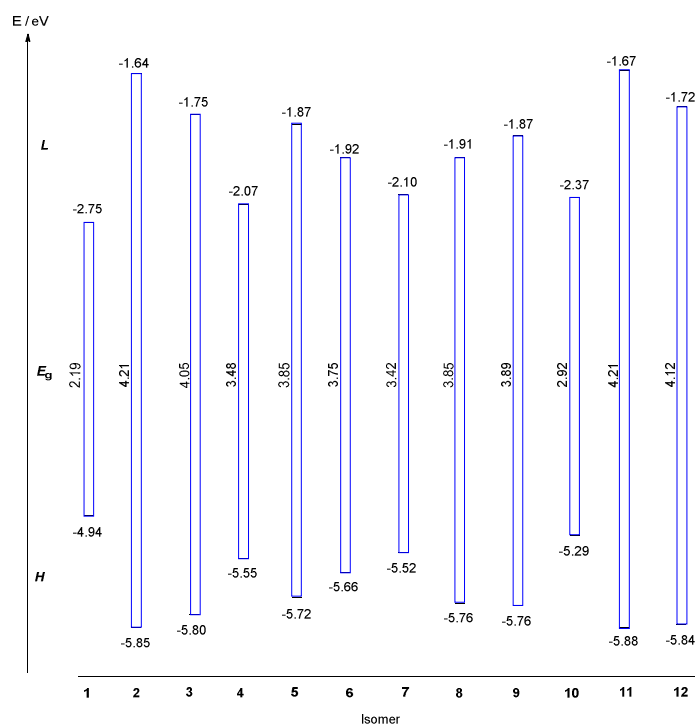
Figure 5. FMO energy diagram of HOMO (H), LUMO (L) and E_g (H-L separation drawn as bars) for all isomers with energies in electron volts (eV).

So far, we have probed the twelve isomers and their various optical properties, leading to trends in stabilities. Now, their ionization energies are investigated with three different types of theories (two DFT, KT and Green's function with the P3 variant). We learnt from the data in Table 1, that long-range functionals such as LC-BLYP overestimates, while pure BLYP underestimates, B3LYP is moderate and similar to that of OVGF, KT is poor and P3 is the

18

most accurate with respect to the experimental value. With this in mind, we now apply these

to focus on calculating the vertical ionization energies that are expected to bracket the

experimental values.

Table 4 shows the vertical ionization energy of the twelve isomers, and lists the pole strengths in parenthesis for OVGF and P3. All of the isomers **2** to **12** show relatively higher vertical ionization energies than pentacene, with values reaching 7.24 eV with **11**, a difference of 1.11 eV. All reproduce the trend that pentacene has the lowest ionization energy, followed closely by isomers **10** and then **4**. Except for pentacene, KT and OVGF give similar values for each isomer, which are on average 0.15 eV greater than the B3LYP functional; the LC-BLYP functional consistently gives the largest IE_Vs, and has a difference to B3LYP between 0.4 and 0.6 eV. The variation between the theories and the isomers are illustrated in Figure 6.

Table 4. 1st Vertical Ionization Energy (IE_V) in electron volts (eV), Calculated with B3LYP, LC-BLYP, Koopmans' Theorem (KT), Outer Valence Green's Function (OVGF) and Third Order Electron Propagator (P3) with their Associated Pole Strengths (PS)

Isomer	B3LYP	LC-BLYP	KT	OVGF	P3
1	6.23	6.65	6.06	6.25 (0.87)	6.51 (0.85)
2	7.20	7.82	7.42	7.37 (0.88)	7.58 (0.86)
3	7.16	7.67	7.31	7.28 (0.88)	7.54 (0.87)
4	6.88	7.44	6.98	7.01 (0.88)	7.24 (0.86)
5	7.07	7.65	7.24	7.20 (0.88)	7.42 (0.86)
6	6.99	7.57	7.16	7.14 (0.87)	7.35 (0.86)
7	6.87	7.40	7.03	6.98 (0.88)	7.29 (0.86)
8	7.12	7.71	7.29	7.25 (0.88)	7.48 (0.86)
9	7.10	7.71	7.28	7.23 (0.88)	7.46 (0.86)
10	6.62	7.11	6.64	6.71 (0.87)	6.94 (0.86)
11	7.24	7.85	7.43	7.39 (0.88)	7.62 (0.86)
12	7.21	7.79	7.38	7.35 (0.88)	7.59 (0.87)

20

In general, the P3 functional gives values that are 0.2 eV greater than the commonly used OVGF functional. The IE_v for picene with P3 is 7.58 eV, which is in excellent agreement with the experimental value at 7.51 eV and suggests that P3 should be given more attention in future studies, particularly due to its level of accuracy over OVGF. The P3 values for isomers **3** (7.54 eV) and **12** (7.59 eV) are remarkably similar to that of picene, while those of **5**, **8** and **9** are similar to each other at 7.44 eV. Both isomers **4** and **6** have relatively low ionization energies (P3) with 7.24 eV and 7.3 eV respectively. Isomer **11** has the greatest IE_v, only slightly larger than picene's theoretical value[65] by 0.06 eV, but significantly greater than pentacene with a difference of 1.11 eV. Isomer **10** is the second lowest at 6.94 eV, after pentacene, but the difference between them is a stabilizing 0.43 eV.
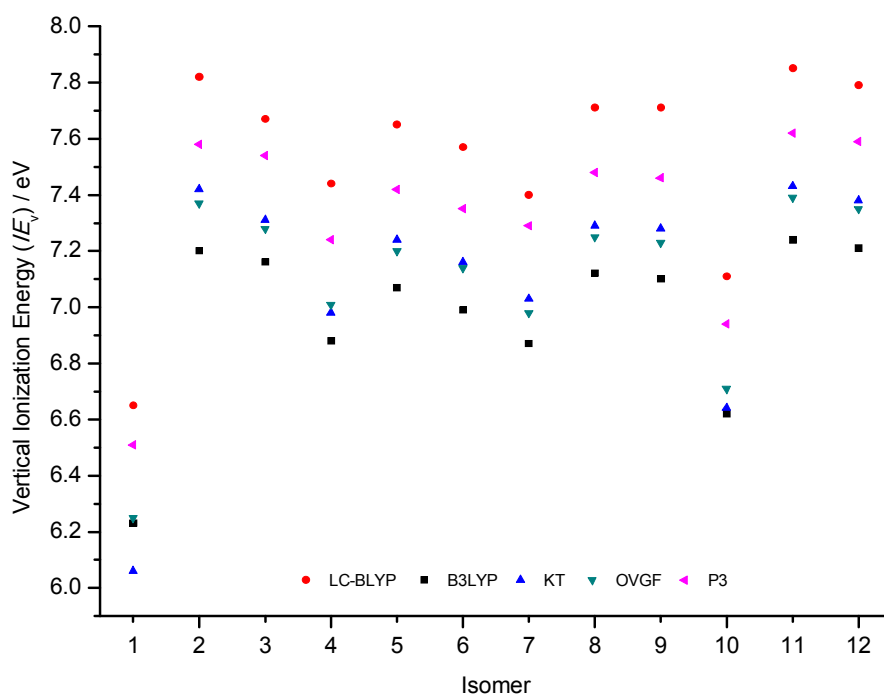
Figure 6. Vertical ionization energies (IE_V) in electron volts (eV) calculated using different theories (LC-BLYP, B3LYP, KT, OVGF, P3) for all isomers.

21

Now we consider (1) the structural relaxation ability of the isomers by calculating their internal hole reorganization energies, (2) their electronic coupling transfer integrals and (3) their rates of charge transfer, for each dimer separation d = 3.0, 3.5 and 4.0 Å, as illustrated in Table 5. The internal hole reorganization energies are overall relatively low, with isomers **4** and **7** to **11** being exceptional between 115 and 143 meV (Figure 7). Relatively high values are observed with **3** (188 meV), **5** (171 meV) and **6** (181 meV), which are similar to that of picene (188 meV); isomer **12** has the highest hole reorganization energy with 212 meV.

Table 5. Hole Reorganization Energy (λ_h / meV) for Each Isomer and the Hole Transfer Integral (t_h / meV) with the Rate of Charge Transfer ($K_{CT} \times 10^{14}$ / s^{-1}) for each Intermolecular Separation of d = 3.0, 3.5 and 4.0 Å

Isomer	λ_h	d = 3.0 Å		d = 3.5 Å		d = 4.0 Å	
		t_h	K_{CT}	t_h	K_{CT}	t_h	K_{CT}
1	97	624	13.022	345	3.968	159	0.841
2	188	147	0.213	144	0.206	141	0.197
3	188	194	0.373	201	0.400	120	0.142
4	122	383	3.433	353	2.918	164	0.632
5	171	205	0.516	205	0.513	162	0.323
6	181	83	0.075	82	0.072	80	0.070
7	133	284	1.627	292	1.715	127	0.326
8	127	242	1.277	244	1.296	159	0.552
9	133	139	0.386	139	0.390	140	0.392
10	115	486	6.082	346	3.087	159	0.653
11	143	20	0.007	18	0.006	23	0.009
12	212	159	0.212	40	0.012	3	0.000
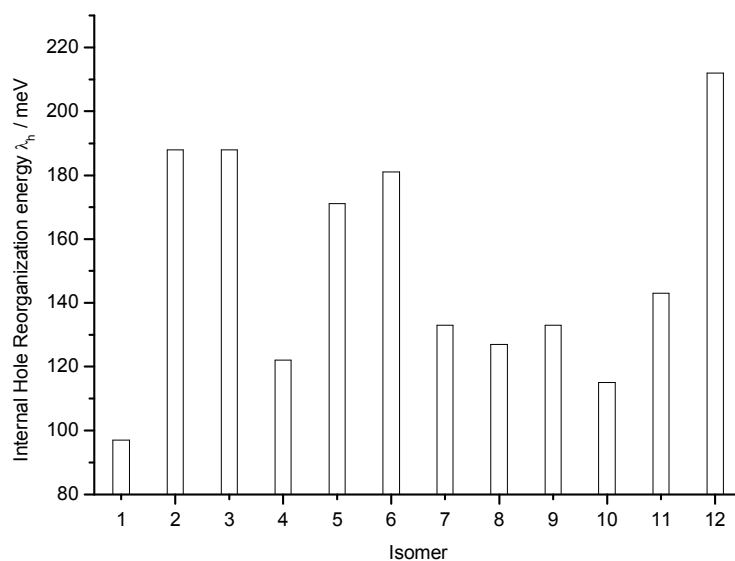
Figure 7. Internal hole reorganization energy (λ_h) in millielectron volts (meV) for each isomer.

Except for pentacene, the hole transfer integrals of the remaining isomers are largely unchanged between the $d = 3.0$ and 3.5 Å separation. The greatest difference is between the $d = 3.5$ and 4.0 Å separation, where the hole transfer integrals are approximately halved. At $d = 3.0$ Å, pentacene has the largest transfer integral at 624 meV, with relatively high values for isomers **4** (383 meV), **7** (284 meV), **8** (242meV) and **10** (486 meV). At $d = 3.5$ Å, these values for the same isomers remain largely unchanged with differences of < 20 meV. At $d = 4.0$ Å, the integral for **7** has decreased by 165 meV, although remarkably, those of isomers **8** and **10** are the same as pentacene at 159 meV, with those of isomers **4** and **5** being even greater at 164 and 162 meV respectively. The relatively strong electronic coupling at this separation may be due to the isomers **4**, **5**, **8** and **10** being both planar and have linear anthracene segments in their structures, with the exceptions being **6** and **9.**

The rates of charge transfer at $d = 3.0$ Å for **4**, **7**, **8** and **10** are exceptional with $K_{CT} = 3.43$, 1.63, 1.28 and 6.08×10^{14} s^{-1} respectively, in comparison to that of pentacene's (13.0×10^{14} s^{-1}); at $d = 3.5$ Å, their rates are of the same order of magnitude at $K_{CT} = 2.92$, 1.72, 1.30 and

23

3.09×10^{14} s^{-1} respectively; those for $d = 4.0$ Å are significantly lower. It is clear these isomers out-perform all other isomers, except for pentacene, with increasing dimer separation. The non-planar isomer **3** has a transfer integral and rate constant of 301 meV and 0.400×10^{14} s^{-1} respectively, which is unexpected given its distorted structure. Those of the other two non-planar isomers **11** and **12** are much less so, with rates up to three orders of magnitude less. The alternative contenders with regards to rates of charge transfer are easily identified from Figure 8, which shows the high-performing values of pentacene at each dimer separation (decreasing from 4.0 to 3.0 Å with increasing t_h) and those of isomers **4**, **7**, **8** and **10** being of the same order of magnitude.
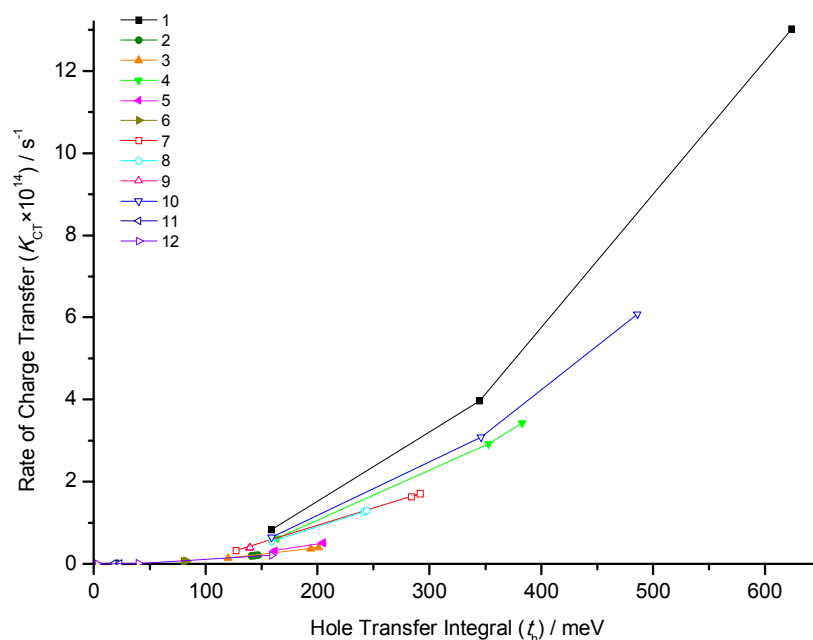
Figure 8. The rate of charge transfer (K_{CT}) versus the hole transfer integral (t_h) in electron volts (meV) for each intermolecular separation ($d = 3.0$, 3.5, 4.0 Å, decreasing separation with increasing transfer integral) for all isomers.

IV. CONCLUSION

This study is the first of its kind to probe the fundamental electronic and optical properties of pentacene's isomers, for both stability and charge transfer in organic electronic applications. Several pure and hybrid functionals were screened for pentacene's FMOs and charge-transfer properties, and the common B3LYP was found to perform the best in comparison to experimental values. Subsequently, the non-planar isomers **3**, **11** and **12** were found to have a relatively similar HOMO to that of picene, while their air stability is nearly two-fold to that of pentacene.

The third order electron propagator (P3) functional gives the most accurate first vertical ionization energy, in comparison to the experimental values of pentacene and picene, and should be used over all other theories for excellent estimates of similar acenes. The isomer **11** was found to have the greatest increase in vertical ionization in comparison to pentacene using P3, by 1.11 eV.

The internal hole reorganization energies of picene and isomer **3** are identical at 0.188 eV, with those of isomers **4**, **7**, **8**, and **10** are less than 0.133 eV. The hole transfer integrals and the rates of charge transfer at three intermolecular separations were evaluated for all isomers and it is no surprise that **4**, **7**, **8**, and **10** have the same order of magnitude as those of pentacene at 3.5 Å, suggesting strong interactions in the solid phase for these molecules. The rates of charge transfer are also exceptional for isomers **4**, **7**, **8** and **10**. Combining these observations with their air stabilities, isomer **8** is the best all-round alternative candidate to pentacene, followed closely by the other three depending on the specific property of interest. Overall, this study shows that the isomers of pentacene deserve attention as potential air-stable and high-performing alternative candidates for organic electronic applications.

25

AUTHOR INFORMATION

Corresponding Author

E-mail: L.Lin@leeds.ac.uk

Author Contributions

The manuscript was written through contributions of all authors. All authors have given

approval to the final version of the manuscript. L Jones and L Lin contributed equally.

The authors declare no competing financial interest.

SUPPORTING INFORMATION

Cartesian coordinates of all optimized and vertical (*i.e.* ionized or electron affinity) structures

for the calculation of the internal hole reorganization energy according to Marcus Theory,

frequency calculations and electronic transitions are available in the Supporting Information.

26

REFERENCES

1   Liu, F.; Xie, L.-H.; Tang, C.; Liang, J.; Chen Q.-Q.; Peng, B.; Wei, W.; Cao, Y.;
     Huang, W. Facile Synthesis of Spirocyclic Aromatic Hydrocarbon Derivatives Based
     on o-Halobiaryl Route and Domino Reaction for Deep-Blue Organic Semiconductors.
     Org. Lett. **2009**, *11*, 3850-3853.

2   Sergeyev, S.; Pisula, W.; Geerts, Y. Discotic Liquid Crystals: A New Generation of
     Organic Semiconductors. *Chem. Soc. Rev.* **2007**, *36*, 1902-1929.

3   Xia, H.; Liu, D.; Xu, X.; Miao, Q. Ambipolar Organic Semiconductors from
     Electron-Accepting Cyclopenta-Fused Anthracene. *Chem. Commun*. **2013**, *49*, 4301-
     4303.

4   Chang, Y.-C.; Kuo, M.-Y.; Chen, C.-P.; Lu, H.-F.; Chao, I. On the Air Stability of
     n-Channel Organic Field Effect Transistors: A Theoretical Study of Adiabatic Electron
     Affinities of Organic Semiconductors. *J. Phys. Chem*. *C* **2010**, *114*, 11595-11601.

5   Bendikov, M.; Wudl, F.; Perepichka, D. Tetrathiafulvalenes, Oligoacenes and their
     Buckminsterfullerene Derivatives: The Brick and Mortar of Organic Electronics. *Chem.
     Rev.* **2004**, *104*, 4891-4945.

6   Forrest, S. The Path to Ubiquitous and Low-Cost Organic Electronic Appliances on
     Plastic. *Nature* **2004**, *428*, 911-918.

7   Logothetidis, S. Flexible Organic Electronic Devices: Materials, Process and
     Applications. *Mat. Sci. Eng. B* **2008**, *152*, 96-104.

8   Klauk, H. *Organic Electronics – Materials, Manufacturing and Applications*; Wiley-
     VCH, Germany, 2006.

27

9   Lewis, J. Material Challenge for Flexible Organic Devices, *Materials Today* **2006**, *9*, 38-45.

10   Brédas, J.-L.; Calbert, J.; Filho, D.; Cornil, J. Organic Semiconductors: A Theoretical Characterization of the Basic Parameters Governing Charge Transport. *PNAS* **2002**, *99*, 5804-5809.

11   Coropceanu, V.; Cornil, J.; Filho, D.; Olivier, Y.; Silbey, R.; Brédas, J.-L. Charge Transport in Organic Semiconductors. *Chem. Rev.* **2007**, *107*, 926-952.

12   Zhu, X.-Y.; Yang, Q.; Muntwiler, M. Charge-Transfer Excitons at Organic Semiconductor Surfaces and Interfaces. *Acc. Chem. Res.* **2009**, *42*, 1779-1787.

13   Jurchescu, O.; Baas, J.; Palstra, T. Effect of Impurities on the Mobility of Single Crystal Pentacene. *Appl. Phys. Lett.* **2004**, *84*, 3061-3063.

14   Nelson, S.; Lin, Y.-Y.; Gundlach, D.; Jackson, T. Temperature-independent Transport in High-Mobility Pentacene Transistors. *Appl. Phys. Lett.* **1998**, *72*, 1884-1856.

15   Klauk, M.; Halik, M.; Zschieschang, U.; Schmid, G.; Radlik, W. High-mobility Polymer Gate Dielectric Pentacene Thin Film Transistors. *J. Apl. Phys.* **2002**, *92*, 5259-5263.

16   Gundlach, D.; Lin, Y.-Y.; Jackson, T.; Nelson, S.; Schlom, D. Pentacene Organic Thin-film Transistors – Molecular Ordering and Mobility. *IEEE Electron Device Letters* **1997**, *18*, 87-89.

17   Lin, Y.-Y.; Gundlach, D.; Nelson, S.; Jackson, T. Stacked Pentacene Layer Organic Thin-film Transistors with Improved Characteristics. *IEEE Electron Device Letters* **1997**, *18*, 606-608.

28

18   Horowitz, G. Organic Field-Effect Transistors. *Adv. Mater.* **1998**, *10*, 365-377.

19   Yamashita, Y. Organic Semiconductors for Organic-field Transistors. *Sci. Technol. Adv. Mater.* **2009**, *10*, 024313-024322.

20   Mitsuhashi, R.; Suzuki, Y.; Yamanari, Y.; Mitamura, H.; Kambe, T.; Ikeda, N.; Okamoto, H.; Fujiwara, A.; Yamaji, M.; Kawasaki, N.; Maniwa, Y.; Kubozono, Y. Superconductivity in Alakali-metal Doped Picene. *Nature* **2010**, *464*, 76-79.

21   Okamoto, H.; Kawasaki, N.; Kaji, Y.; Kubozono, Y.; Fujiwara, A.; Yamiji, M. Air-assisted High-performance Field-effect Transistor with Thin Films of Picene. *J. Am. Chem. Soc.* **2008**, *130*, 10470-10471.

22   Wang, Y.; Motta, S.; Fabrizia, N.; Friedlein, R. Effect of Oxygen on the Electronic Structure of Highly Crystalline Picene Films. *J. Am. Chem. Soc.* **2011**, *133*, 10054-10057.

23   Mitrofanov, O.; Lang, D.; Kloc, C.; Wikberg, J.; Siegrist, T.; So, W.-Y.; Sergent, M.; Ramirez, A. Oxygen-related Band Gap State in Single Crystal Rubrene. *Phys. Rev. Lett.* **2006**, *97*, 16660.

24   Lu, C.-K.; Meng, H.-F. Hole Doping by Molecular Oxygen in Organic Semiconductors: Band-structure Calculations. *Phys. Rev. B* **2007**, *75*, 235206.

25   Najafov, H.; Mastrogiovanni, D.; Garfunkel, E.; Feldman, L.; Podzorov, V. Photon-assisted Oxygen Diffusion and Oxygen-related Traps in Organic Semiconductors. *Adv. Mater.* **2011**, *23*, 981-985.

26   Nguyen, T.; Shim, J.; Lee, J. Density Functional Theory Studies of Hole Mobility in Picene and Pentacene Crystals. *J. Phys. Chem. C* **2015**, *119*, 11301-11310.

29

27   Pelzer, K.; Greenman, L.; Gidofalvi, G.; Mazziotti, D. Strong Correlation in Acene Sheets from the Active-space Variational Two-electron Reduced Density Matrix Method: Effects of Symmetry and Size. *J. Phys. Chem. A* **2011**, *115*, 5632-5640.

28   Aihara, J.-i. Dimensionality of Aromaticity. *Bull. Chem. Soc. Jpn.* **2008**, *81*, 241-247.

29   Matsumoto, T.; Nagashima, U.; Tanabe, K.; Ono, S. Materials Design of Lithium Ion Rechargeable Battery by Quantum Chemical Calculation – Search of Specific Carbon Structure Models. *J. Comput. Chem. Jpn.* **2003**, *2*, 63-70.

30   Vasu, D.; Yorimitsu, H.; Osuka, A. Palladium-Assisted "Aromatic Metamorphosis" of Dibenzothiophenes into Triphenylenes. *Angew. Chem. Int. Ed*., **2015**, *54*, 7162-7166

31   Iwasaki, M.; Araki, Y.; Lino, S.; Nishihara, Y. Synthesis of Multisubstituted Triphenylenes and Phenanthrenes by Cascade Reaction of *o*-Iodobiphenyls of (z)-β-Halostyrenes with *o*-Bromobenzyl Alcohols through Two Sequential C-C Bond Formations Catalyzed by a Palladium Complex. *J. Org. Chem*., **2015**, 80, 9247-9263.

32   Hanwell, M.; Curtis, D.; Lonie, D.; Vandermeersch, T.; Zurek, E.; Hutchison, G. Avogadro:An Advanced Semantic Chemical Editor, Visualization and Analysis Platform. *J. Cheminformatics.* **2012**, *4*.

33   Gaussian 09, Revision D.01, Frisch, M. J.; Trucks, G. W.; Schlegel, H. B.; Scuseria, G. E.; Robb, M. A.; Cheeseman, J. R.; Scalmani, G.; Barone, V.; Mennucci, B.; Petersson, G. A.; *et al.* Gaussian, Inc., Wallingford CT, 2009.

34   Langhoff, S. Theoretical Infrared Spectra for Polycyclic Aromatic Hydrocarbon Neutrals, Cations, and Anions. J. *Phys. Chem*, **1996**, *100*, 2819-2841.

35   Hosoi, Y.; Okamura, K.; Kimura, Y.; Ishii, H.; Niwano, M. . *Applied Surface Science*,
2005, *244*, 607-610.

36   Sancho-García, J.; Pérez-Jiménez, A. Charge-Transport Properties of Prototype
Molecular Materials for Organic Electronics Based on Graphene Nanoribbons. *Phys.
Chem. Chem. Phys.*, **2009**, 11, 2741-2746.

37   Cappellini, G.; Malloci, G.; Mulas, G. Electronic Excitations of Oligoacenes: A Time
Dependent Density Functional Theory Study. *Superlattices and Microstructures*, **2009**,
46, 14-18.

38   Malloci, G.; Mulas, G; Cappellini, G.; Joblin, C. Time-Dependent Density Functional
Theory of the Electronic Spectra of Oligoacenes in the Charge States -1, 0, +1 and +2.
Chemical Physics, **2007**, *340*, 43-58.

39   Malloci, G.; Cappellini, G.; Mulas, G; Mattoni, A. Electronic and Optical Properties of
Families of Polycylic Aromatic Hydrocarbons: A Systematic (Time-Dependent)
Density Functional Theory Study. *Chemical Physics*, **2011**, *384*, 19-27.

40   Hu, Y.; Yin, J.; Chaitanya, K.; Ju, X.-H. Theoretical Investigation on Charge Transfer
Properties of 1,3,5-Tripyrrolebenzene (TPB) and its Derivatives with Electron-
Withdrawing Substituents. *Croat. Chem. Acta.*, **2016**, *89*, 81-90.

41   Viani, L.; Olivier, Y.; Athanasopoulos, S.; da Silva Filho, D.; Hulliger, J.; Brédas, J.-L.;
Gierschner, J.; Cornil, J. Theoretical Characterization of Charge Transport in One-
Dimensional Collinear Arrays of Organic Conjugated Molecules. *Chem. Phys. Chem.*,
2010, *11*, 1062-1068.

31

42   Baumeier, B.; Kirkpatrick, J.; Andrienko, D. Density-Functional Based Determination of Intermolecular Charge Transfer Properties for Large-Scale Morphologies. *Phys. Chem. Chem. Phys.*, **2010**, *12*, 11103-11113.

43   Mannsfeld, S.; Virkar, A.; Reese, C.; Toney, M.; Bao, Z. Precise Structure of Pentacene Monolayers on Amorphous Silicon Dioxide and Relation to Charge Transport. *Adv. Mater.*, **2009**, *21*, 2294-2298.

44   Winkler, M.; Houk, K. Nitrogen-rich Oligoacene: Candidates for n-channel Organic Semiconductors. *J. Am. Chem. Soc.* **2007**, *129*, 1805-1815.

45   Hutchison, G.; Ratner, M; Marks, T. Hopping Transport in Conductive Heterocyclic Oligomers: Reorganization Energies and Substituent Effects. *J. Am. Chem. Soc.* **2005**, *127*, 2339-2350.

46   Newman, C; Frisbie, C.; Filho, D.; Brédas, J.-L.; Ewbank, P.; Mann, K. Introduction to Organic Thin-film Transistors and Design of n-channel Organic Semiconductors. *Chem. Mater.* **2004**, *16*, 4436-4451.

47   Sancho-García, J.; Pérez-Jiménez, A. A Theoretical Study of π-Stacking Tetracene Derivatives as Promising Organic Molecular Semiconductors. *Chemical Physical Letters*, **2010**, *499*, 146-151.

48   Cardia, R.; Malloci, G.; Bosin, A.; Serra, G.; Cappwllini, G. Computational Investigation of the Effects of Perfluorination on the Charge-Transport Properties of Polyaromatic Hydrocarbons. *Chemical Physics*, **2016**, *478*, 8-13.

32

49　Sabirov, D. A Correlation Between the Mean Polarizability of the "Kinked" Polycyclic Aromatic Hydrocarbons and the Number of H…H Bond Critical Points Predicted by Atoms-In-Molecules Theory. *Comput. Theor. Chem.* **2014**, *1030*, 81-86.

50　Refaely-Abramson, S.; Beer, R.; Kronik, L. Fundamental and Excitation Gaps in Molecules of Relevance for Organic Photovoltaics from an Optimally Tuned Range-separated Hybrid Functional. *Phys. Rev. B* **2011**, *84*, 075144.

51　Sjoberg, P.; Murray, J.; Brinck, T.; Politzer, P. Average Local Ionization Energies on the Molecular Surfaces of Aromatic Systems as Guides to Chemical Reactivity. *Can. J Chem*. **1990**, *68*, 1440-1443.

52　Koopmans, T. Über die Zuordnung von Wellenfunktionen und Eigenwerten zu den Einzelnen Elektronen Eines Atoms. *Physica* **1934**, *1*, 104-113.

53　Kishimoto, N.; Hagihara, Y.; Ohno, K.; Knippenberg, S.; Francois, J.-P.; Deleuze, M. Probing the Shape and Stereochemistry of Molecular Orbitals in Locally Flexible Aromatic Chains: A Penning Ionization Electron Spectroscopy and Green's Function Study of the Electronic Structure of Biphenyl. *J. Phys. Chem. A* **2005**, *109*, 10535-10546.

54　Onida, G.; Reining, L.; Rubio, A. Electronic Excitations: Density-functional Versus Many-body Green's-function Approaches. *Rev. Mod. Phys.* **2002**, *74*, 601.

55　Niehaus, T.; Rohlfing, Sala, F.; Carlo, A.; Frauenheim, Th.; Quasiparticle Energies for Large Molecules: A Tight-binding based Green's-function Approach. *Phys. Rev. A*, **2005**, *71*, 022508.

56 Danovich, D.; Green's Function Methods for Calculating Ionization Potentials, Electron Affinities, and Excitation Energies. *Wiley Interdisciplinary Reviews: Computational Molecular Science*. **2011**, *1*, 377-387.

57 Dolgounitcheva, O.; Díaz-Tinoco, M.; Zakrzewski, V.; Richard, R.; Marom, N.; Sherrill, C.; Ortiz, J. Accurate Ionization Potentials and Electron Affinities of Acceptor Molecues IV: Electron-propagator Methods. *J. Chem. Theory. Comput.* **2016**, *12*, 627-637.

58 Corzo, H.; Galano, A.; Dolgounitcheva, O.; Zakrzewski, V.; Ortiz, J. NR2 and P3+: Accurate, Efficient Electron-propagator Methods for Calculating Valence, Vertical Ionization Energies of Closed-shell Molecules. *J. Phys. Chem. A* **2015**, *119,* 8813-8821.

59 Díaz-Tinoco, M.; Dolgounitcheva, O.; Zakrzewski, V.; Ortiz, J. Composite Electron Propagator Methods for Calculating Ionization Energies. *J. Chem. Phys.* **2016**, *144,* 224110.

60 Wang, C.; Dong, H.; Hu, W.; Liu, Y.; Zhu, D. Semiconducting π-conjugated Systems in Field-effect Transistors: A Material Odyssey of Organic Electronics. *Chem. Rev.* **2012**, *112,* 2208-2267.

61 Djurovich, P.; Mayo, E.; Forrest, S.; Thompson, M. Measurement of the Lowest Unoccupied Molecular Orbital Energies of Molecular Organic Semiconductors. *Org. Elec.* **2009**, *10*, 515-520.

62 Gruhn, N.; Filho, D.; Bill, T.; Malagoli, M.; Coropceanu, V.; Kahn, A.; Brédas, J.-L. The Vibrational Reorganization Energy in Pentacene: Molecular Influences on Charge Transport. *J. Am. Chem. Soc.* **2002**, *124*, 7918-7919.

34

63   Sancho-García, J. Assessment of Density-Functional Models for Organic Molecular Semiconductors: The Role of Hartree-Fock Exchange in Charge-Transfer Process. *Chemical Physics*, **2007**, *331*, 321-331.

64   Sancho-García, J.; Pérez-Jiménez. Theoretical Study of Stability and Charge-Transport Properties of Coronene Molecules and Some of its Halogenated Derivatives: A Path to Ambipolar Organic-Based Materials. *J Chem. Phys.*, **2014**, *141*, 134708.

65   Modelli, A.; Musson, L. Rapid Quantitative Prediction of Ionization Energies and Electron Affinities of Polycyclic Aromatic Hydrocarbons. *Chemical Physics*, **2007**, *332*, 367-374.

66   Kivelson, S.; Chapman, O. Polyacene and a New Class of Quasi-one-Dimensional Conductors. *Phys. Rev. B*, **1983**, *28*, 7236.

67   McMahon, R.; Chapman, O. Triplet Ground-State Cycloheptatrienylidene. *J. Am. Chem. Soc.*, **1986**, *108*, 1713-1714

68   Nendel, M.; Houk, K.; Tolbert, L.; Vogel, E.; Jiao, H.; von Ragué Schleyer, P. The Bond Localization Energies in the Aromatic Bismethano[14]annulenes. *Angew. Chem. Int. Ed. Engl.*, **1997**, *36*, 748-750.

69   Bendikov, M.; Duong, H.; Starkey, K.; Houk, K.; Carter, E.; Wudl, F. Oligoacenes: Theoretical Prediction of Open-Shell Singlet Diradical Ground States. *J. Am. Chem. Soc.*, **2004**, *126*, 7416-7417.

35

Table of Contents Graphic (TOC)

Isomeric Pool of
12 $C_{22}H_{14}$ Acenes

FMO Energies
Ionization Energies
Reorganization Energies
Transfer Integrals
Rates of Charge Transfer

Benzo[*b*]chrysene
(planar)

Naphtho[*c*]phenanthrene
(non-planar)

**Air-Stable and High Charge-Transfer
Alternative Candidates to Pentacene**

Dibenzo[*a,c*]anthracene
(planar)

Benzo[*a*]tetracene
(planar)

36